Porous materials of electrochemical cells in the CAE design process

Poröse Materialien elektrochemischer Zellen im CAE-Design-Prozess

S. Fell[1], **K. Steiner**[2], **A. Latz**[2], **J. Zausch**[2], **J. Becker**[2], **G. B. Less**[3], **J. H. Seo**[3], **S. Han**[3], **A. M. Sastry**[3]

[1]Adam Opel GmbH, Rüsselsheim, Germany, [2]Fraunhofer ITWM, Kaiserslautern, Germany, [3]University of Michigan, Ann Arbor, U.S.A.

Abstract

For the development of sustainable mobility electrochemical cells, especially the Polymer Electrolyte Membrane (PEM) fuel cell and the secondary Li-ion cell represent an important technology to enable highly efficient electric powertrains.

Major components of these electrochemical cells consist of porous, composite materials comprised of electrically or ionically conducting and non-conducting (neither electrically nor ionically) materials. Furthermore, some of the conductive materials are electrochemically active. The multiple and complex charge, mass and heat transport as well as the mass conversion mechanisms taking place on the surfaces and in the solid and pore structures of these materials need to be balanced and optimized for an efficient conversion of chemical energy into electrical energy. But an efficient energy conversion can be assured only if the transport and reaction process in association with the microstructural morphology and its fabrication of the porous, composite material are understood.

By the examples of the electrochemically inactive micro-porous layer of fuel cell diffusion media and the electrochemically active porous Li-ion battery electrode, a computational aided engineering (CAE) process for material design and optimization is described. In a figurative sense such a process offers the possibility to perform computational analysis of the porous type electrochemical *"combustion chamber",* the already established standard for the development of traditional combustion engines.

Kurzfassung

Für die Entwicklung einer nachhaltigen Mobilität sind elektrochemische Zellen, insbesondere die Polymer Elektrolyte-Membran-(PEM)-Brennstoffzelle und die sekundäre (aufladbare) Li-Ionen-Batterie, entscheidende Technologien zur Realisierung hoch effizienter, elektrischer Antriebsstränge.

Wesentliche Komponenten dieser elektrochemischen Zellen sind aus porösen Kompositmaterialien aufgebaut, bestehend aus einer soliden (elektrisch leitend) und einer Elektrolytphase (Ionen leitend). Diese Materialien können in elektrochemisch aktive und inaktive Materialien klassifiziert werden und werden im Allgemeinen eingesetzt zur Maximierung des Kontakts (erhöhte Oberfläche) und zur Minimierung des Transportwiderstandes (verkürzte Diffusionslängen) zwischen den Reaktionspartnern, der soliden und der Elektrolytphase für eine effiziente Umwandlung von chemischer in elektrische Energie. Aber diese effiziente Energieumwandlung kann nur sichergestellt werden, wenn die Transport- und Reaktionsprozesse in Verbindung mit der Mikromorphologie und dem Herstellungsprozess des porösen Kompositmaterials sehr gut verstanden sind.

Am Beispiel der elektrochemisch inaktiven mikroporösen Sicht des Diffusionsmaterials einer PEM-Brennstoffzelle und der elektrochemisch aktiven Elektrode einer Li-Ionen-Zelle wird ein CAE-Design-Prozess zur Materialoptimierung dargestellt. Im übertragenen Sinne ermöglicht der dargestellte Prozess die rechnerische Analyse des porösen, elektrochemischen „Brennraums“, den bereits etablierten Standard für die traditionellen Verbrennungsmotoren.

1 Introduction

As electrochemical energy converter the PEM fuel cell as well as the Li-ion battery is considered as enabler for highly efficient electric powertrains. But unfortunately there are still some gaps to close with regard to the challenging automotive requirements due to cost, performance, reliability and durability although significant efforts have been taken over the past few years **[1, 2]**.

Because the energy conversion of an electrochemical cell takes place in nano- and/or micro-porous composite materials in contrast to conventional thermal engines, these porous materials ─ classified into electrochemically active and inactive materials ─ need to be improved in order to close these gaps. Hence, a renewed focus of efforts is required to develop materials and fundamental material understanding to assure long-term durability and reliability of electrochemical cells. Driven by the current understanding that heat, mass and charge transport inside the porous multi-functional layers strongly impact the performance and durability of electrochemical cells, this paper introduces a CAE process to support the experimental material development process by simulation.

The paper starts with some basic principles and a description of the applied porous composite materials in a fuel cell (Chapter 2) and Li-ion battery (Chapter 3). Then, Chapter 4 specifies the CAE process and Chapter 5 and 6 concentrate on two examples of modeling

porous materials. Chapter 5 deals with the electrochemically inactive porous structure of the microporous layer of PEM fuel cell diffusion media while Chapter 6 covers the electrochemically active electrode of a Li-ion cell. Finally, Chapter 7 summarizes the methodology and points out challenges, limitations and new possibilities by applying the described material level CAE process.

2 Fuel Cell Principle and Porous Materials

The basic design of a PEM fuel cell involves two gas diffusion electrodes on either side of a polymer electrolyte. Hydrogen and oxygen pass over each of the electrodes and through means of electrochemical reactions, electricity, heat and water are produced. Hydrogen fuel is supplied to the anode of the fuel cell while oxygen is supplied to the cathode. Through an electrochemical reaction, the hydrogen molecule splits into two electrons and two protons. Each takes a different path to the cathode. The electrons are capable of taking a path other than through the electrolyte, which, when harnessed correctly, can produce electricity for a given load (e.g. an electric motor in an automobile). The proton passes through the electrolyte and both are reunited at the cathode. There the electrons, protons, and oxygen combine to form water.

Porous materials (diffusion media and catalysts layer) have numerous functions in a PEM fuel cell. They act as a transport media for reactant species, reaction products, electric current and heat and provide the large surface area for the electrochemical reaction (**Figure 1**).

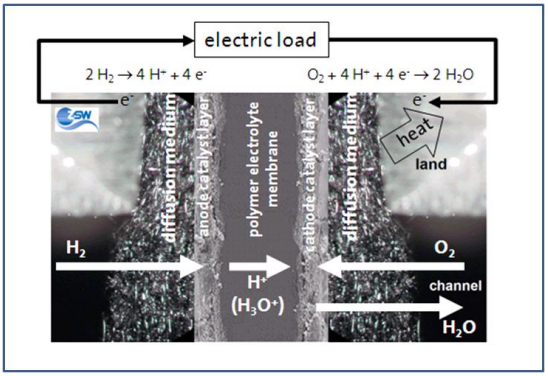

Figure 1: Porous materials in a PEM fuel cell and basic transport processes (Source: ZSW Ulm, Germany).

Traditionally, PEM fuel cell diffusion media have been made of carbon fiber paper (CFP) or felt treated with PTFE or similar fluorocarbons to render the surfaces hydrophobic, i.e. to ensure that water does not fill up all the pores **[3]**. The porous nature of these materials allows the reactants to access those parts of the electrodes that are under the flow channel

ridges, and provides a passage for reaction product water from the electrode to the flow channel. The transport of the gaseous species is dominantly driven by diffusion, and movement of liquid water takes place by capillary action **[4, 5]**. The solid fraction of the porous diffusion medium on the other hand connects the current and heat generating electrodes with the bipolar plate electronically and thermally, i.e. the electric current as well as the heat is conducted through the diffusion medium. To provide a well-defined interface between the macroporous fiber paper and the nanoporous gas diffusion electrode a so-called microporous layer coating (MPL) is typically applied onto the fiber paper (**Figure 2)**. Made from carbon particle aggregates that are bound together with polymer additives which also render the microporous layer hydrophobic, this layer is speculated to act as a check valve for liquid water to prevent flooding of the gas diffusion electrode. The gas diffusion electrode, finally, is a porous layer itself comprising the catalyst, which is typically platinum on a carbon support, as well as ionomer and hydrophobic binder.

The primary functions of porous media in a fuel cell are mass, charge and heat transport and mass conversion. A descriptive model has to reflect all these functions and processes. Depending on the relevant structural scales and the processes taking place in the individual layers, the relevant physics may differ for the different porous materials. For instance, the pore sizes in the fiber paper are on the 10 µm scale which justifies using continuum physics to describe gas transport, whereas the pore sizes of the microporous layer and the gas diffusion electrode are rather in the 10 nm scale which requires the consideration of particle-wall interactions. This circumstance will be further discussed in Chapter 5.

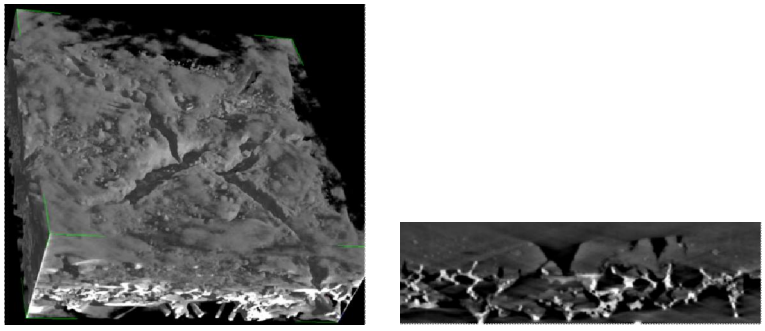

Figure 2: 3D tomographical view of a representative PEM fuel cell diffusion medium (left) and 2D slice thereof (right). The MPL may form a distinct layer on the CFP or, like in this case, form a complex and dense or cracked penetration profile in the CFP (source: Opel).

3 Li-ion Battery Principle and Porous Materials

The traditional design of a Li-ion battery is illustrated in **Figure 3.** Briefly, the cell is comprised of an aluminum foil current collector supporting a porous composite cathode, an electrolyte, and a porous composite anode supported on a copper foil current collector. The two electrodes are separated by an electronically insulating porous membrane filled with ion-conducting electrolyte.

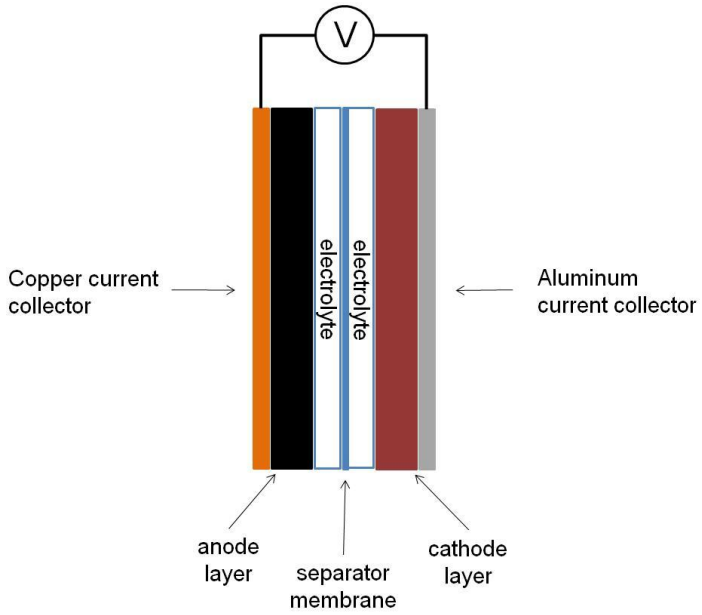

Figure 3: A schematic representation of a typical Li-ion battery. Note that anode, cathode and separator membranes are all porous materials.

The composite electrodes are a mixture of an electroactive material, a polymeric binder and a conductive additive. In cathodes the active materials are transition metal compounds; the most common in the current generation of batteries are lithium manganese oxide, lithium iron phosphate, and blended metal oxides. The anodes are most usually graphitic materials, though there has been promising research into the use of lithium titanium oxide and silicon as anode materials. **Figure 4** shows the 3D view of a tomographical imaging data set of a representative negative electrode indicating the complex particle and pore shape of the comparatively dense porous material **[6]**.

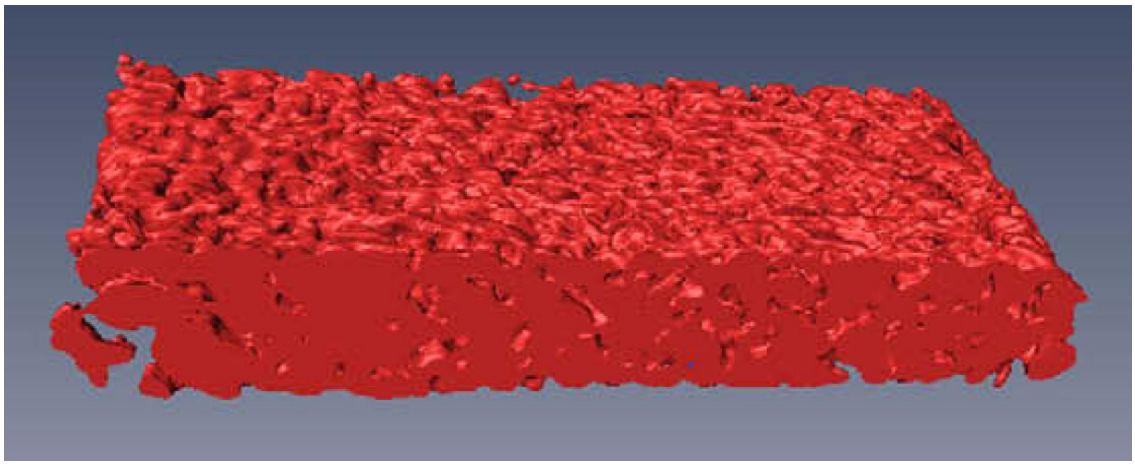

Figure 4: 3D view of a tomographical imaging data set of a typical graphite negative electrode having the dimension of 43x348x144 μm^3 **[6]**.

During normal discharge of a Li-ion battery, Li^+ exits the anode and travels through the electrolyte to the cathode where it is intercalated into the crystal lattice of the active material. The Li^+ ion follows the reverse path during the charging process. The addition or loss of the Li-ion to the electrodes is accompanied by a RedOx reaction whereby an electron is gained or lost by the active material. During discharge when the Li^+ exits the anode, the anode gains an electron which is taken by the external circuit and provided to the cathode which is oxidized during the intercalation of the ions. The electrons traveling through the external circuit can be harnessed to do work as necessary. The electrolyte, typically an organic carbonate solution of $LiPF_6$, is electronically insulating but ionically conductive.

Modeling of Li-ion batteries has been an ongoing research effort for a number of years now. The different approaches in literature can be categorized into continuum models **[7 - 10]**, low-dimensional porous models **[11 - 13]** and multi-scale, multi-physics models based on 3D images of real electrode structures **[14 - 29]**. The latter approach allows simulation of micro- (i.e. local) distributions of variables (ionic concentration, potential, etc.) in 3D at the cost of computational time. The 1D, 2D and continuum models are faster than the 3D models, but only simulate macro- (i.e. averaged) distributions of variable properties. The multi-scale, multi-physics models **[14 - 29]** began by interrogating the percolation statistics of the ideal aspect ratios and packing densities of ellipsoidal particles, fibers, and deformed fibers in order to form a continuous network in three dimensions, a necessary condition for a composite electrode. The physics of percolation influences the formation and aspect ratios of larger aggregates **[16]** of these particles; accurate 3D geometry and dimensionality of the aggregates yields a basis for developing predictive models that bridge the gap between

chemical modeling and nanoparticle interaction **[30 - 32]**. A thermodynamically consistent transport model of Li-ion batteries on the micro-structural level of the pores is presented in **[33]**. Multi-scale, multi-physics modeling enables the interrogation of the disparate size (atomic to macro) and time (seconds to minutes) scales present in a battery system.

4 CAE Process for Porous Materials of Electrochemical Cells

With respect to characterization, specification and modeling, the porous, composite materials of electrochemical cells are typically treated macroscopically from the perspective of their effective properties. However, the macroscopic behavior of the porous material is determined by

- the micro-/nanoporous geometric morphology,
- the composition of the solid and/or electrolyte phase,
- the physical behavior of the individual phases,
- the electrochemical energy release, and
- the momentum, mass, heat, and charge transport processes in the individual phases.

Currently there is a lack of understanding of the correlation between “microscopic” material manifestation and macroscopic effective properties. Therefore, costly and time-consuming experimental “trial and error” approaches are necessary to meet the desired combination of macroscopic material specifications. The goal of current development efforts is to generate a model understanding of mechanisms that determine macroscopic material properties and/or to tailor materials to specifications in a virtual material design cycle **[34]**.

The proposed material design CAE process for porous materials comprises four major steps (**Figure 5**) **[35]**:

I. Imaging of the material's pore structure (imaging)
II. Create a digitized 3D image of the porous material (virtual material)
III. Describe transport processes within the material structure, predict macroscopic properties and run virtual iteration loops with virtual material modifications to optimize properties (simulation)
IV. Recommend material manifestations, fabricate material and provide fabricated material to imaging to check achieved properties, i.e. back to I. (material specifications)

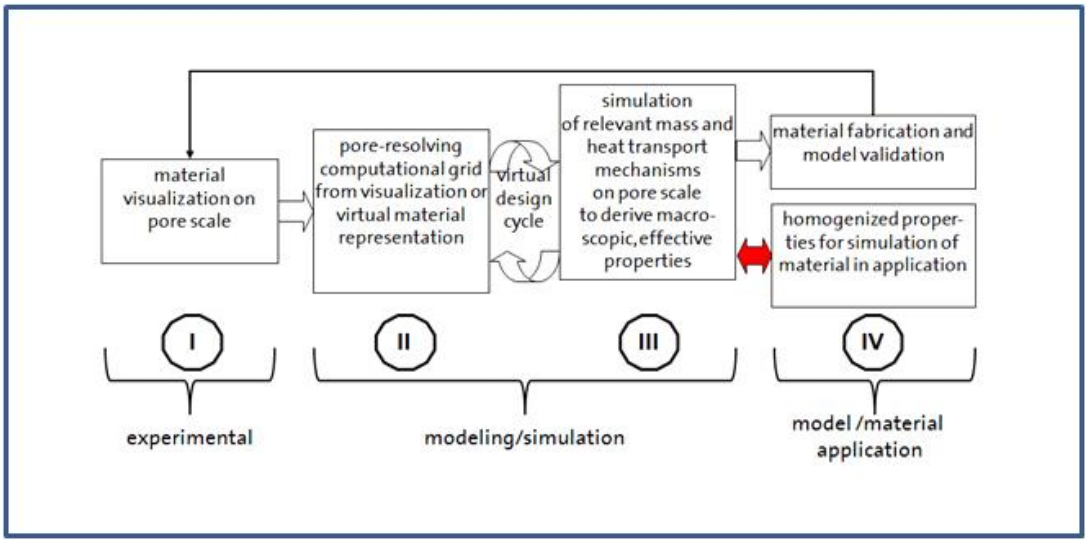

Figure 5: Schematic description of a material design cycle.

Using the example of the electrochemical inactive porous structure of the micro porous layer of the diffusion media of a PEM fuel cell and the electrochemical active electrode of a Li-ion cell the CAE process is demonstrated in the following chapters.

For examples where the material design cycle is described and applied please see **[34, 36-38]**.

5 Modeling of the Electrochemical Inactive Microporous Layer of the Gas Diffusion Layer of a Fuel Cell

The starting point of the modeling process (as described by Step II in **Figure 5**) is the construction of a 3D pore structure model. For this purpose, the software GeoDict **[39]** was used. GeoDict allows to import 3D tomography images and to create models virtually. The virtual material design process with GeoDict was successfully established for fibrous gas diffusion layers (see **[40, 41]**) to optimize the two-phase behavior of diffusivity and permeability. Since suitable 3D imaging data sets of MPL are not available yet, the pore structure model has to be constructed virtually:

A micro porous layer (MPL) consists of agglomerates of carbonized particles. **Figure 7** (right) gives an impression of the surface of such an MPL. The base material used in the manufacturing of this layer is acetylene black, which exhibits primary particle sizes of ~ 50 nm and forms agglomerates of approx. 200 particles **[42]**.

This information can be used in the virtual construction process: a single agglomerate is described by 200 slightly overlapping spheres. The arrangement of the spheres is randomly, but two neighboring spheres may overlap by 2 to 22 nm. **Figure 6** shows two agglomerates created in this way.

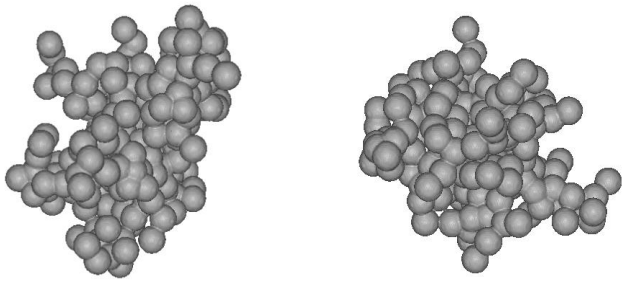

Figure 6: Agglomerates consisting of 200 spheres with diameter 52 nm.

Such agglomerates are then randomly placed in the 3D model volume until the desired porosity is reached. **Figure 7** shows a resulting 3D voxel mesh in comparison with the SEM image. Besides the visual similarity, the consistency of the virtual model with the real medium was checked by calculating the pore size distribution of the virtual model and comparing the results with measurements **[38]**.

But – to enter the virtual design cycle – not only a reconstruction of the real media is of interest. It is additionally necessary to be able to vary construction parameters and to

observe the influence of these variations in the effective material properties. Exemplarily, **Figure 8** shows MPL structures created with different parameters.

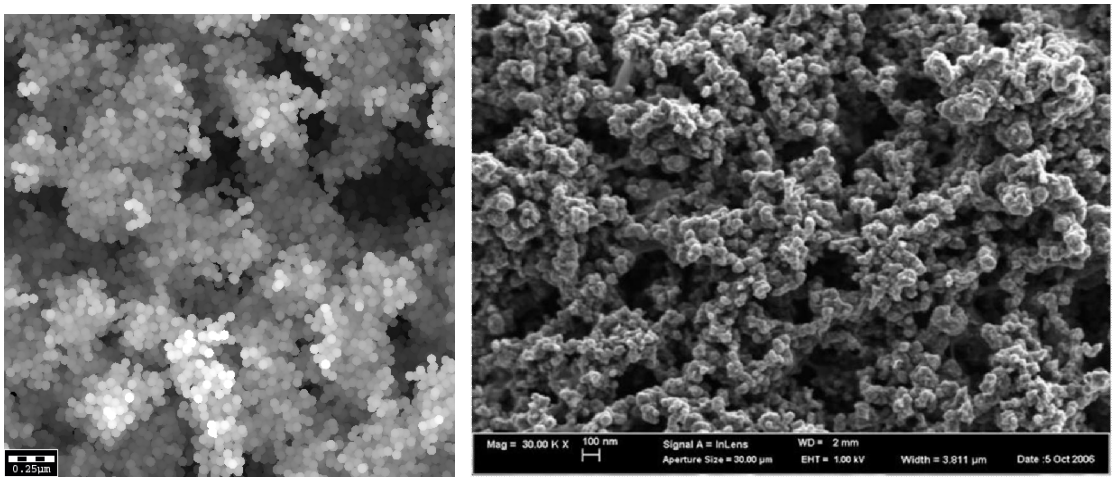

Figure 7: Comparison of a surface of a virtually generated MPL with porosity 55% (left) with an SEM image of an MPL surface (right).

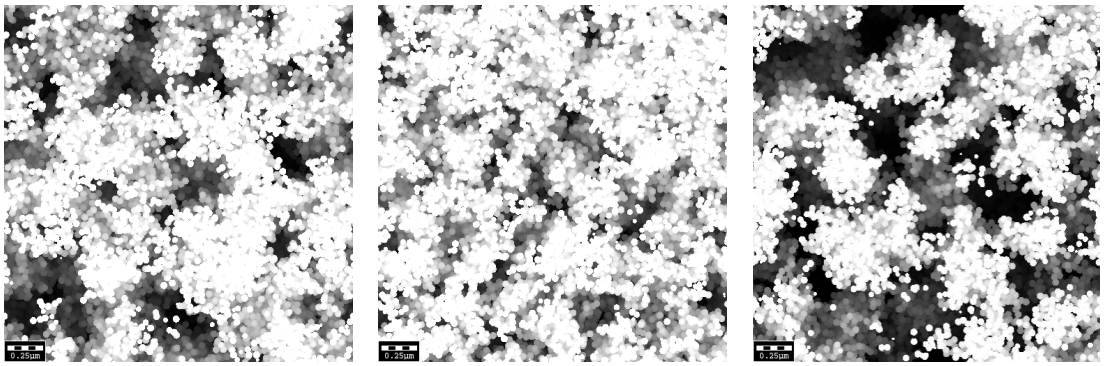

Figure 8: Cross sections of virtual MPL structures created with different parameters: left: porosity 55%, agglomerates of 200 spheres, center: porosity: 55%, agglomerates of 50 spheres, right: porosity 70%, agglomerates of 200 spheres. Other parameters are identical.

The resulting 3D voxel meshes can then be used to calculate the effective properties of the MPL (Step III of **Figure 5**). This can again be done with GeoDict. Besides the purely geometrical attributes like pore size distribution and surface area one is interested in the transport properties of the layer. As transport inside the MPL is governed by diffusive processes, the effective diffusivity of the porous layer is of special interest.

For porous media, the usual approach to calculate the (bulk) diffusivity is to neglect Knudsen effects and to solve the Laplace equation $-\Delta c = 0$ in the pore space with no-flux boundary

conditions on the solid surfaces and a concentration drop in one space direction as boundary conditions **[43]**. In this way, the total diffusion flux j is determined numerically and with Fick's first law $j = -D_{bulk} \nabla c$ the diffusivity D_{bulk} is found.

But pore sizes inside the MPL are of the same order of magnitude as the mean free path of the gas. Thus, Knudsen effects have to be taken into account. This can be done by applying Bosanquet's formula $\mathrm{D} = \left(\mathrm{D}_{\mathrm{Bulk}}^{-1} + \mathrm{D}_{\mathrm{Kn}}^{-1} \right)^{-1}$, where the effective bulk diffusivity can be calculated as described above. Basically, the transport resistance can be considered as a parallel circuit of the Bulk and the Knudsen type of mass transport resistance. To determine D_{Kn}, a random walk method can be used **[44]**. The overall approach is implemented in GeoDict and was developed and applied in a joint Opel/Fraunhofer ITWM effort to determine the effective diffusivity of the MPL numerically. For O_2 in N_2 at standard conditions (25°C, 1013 mbar), the resulting Knudsen diffusivity equals around 50% of the Bulk diffusivity number. For more technical details please see **[38]**.

6 Modeling of the Electrochemically Active Li-ion Electrode

In the present chapter, the starting point of Step II of **Figure 5** is a simple, generic Li-ion cell simulated by the software OpelLiB, developed jointly with Fraunhofer ITWM. OpelLiB is designed as a tool to simulate both charge and ion transport in the electrodes as well as the separator of Li-ion batteries including the linkage to the material micro-morphology design capabilities of GeoDict **[39]**. The microstructure of the electrodes will be resolved on micrometer scale. On this scale the transport in the active particle and the electrolytes in between the particles has to be considered separately.

In this case the cell is comprised of a lithium manganese oxide cathode, a lithium metal anode, and a 1.2 M $LiPF_6$ electrolyte solution in EC:DMC (3:7 v/v). In the modeled cell there are four cubical-shaped cathode particles represented by squares of dimensions 25 μm x 25 μm x 12.5 μm, and nine cubical-shaped anode particles; four of dimensions 15 μm x 15 μm x 25 μm and five of dimensions 15μm x 15μm x 50μm. The cell was discharged at 1C, 2C, 3C and 4C where C = 16.5 nA. In each case the initial states of charge were 0.56 and 0.17 for the anode and cathode, respectively.

The boundary conditions used in the isothermal simulations are as follows: the concentration boundary condition is a Neumann-type zero flux at the electrode current collector interface of both anode and cathode, the potential boundary condition at the anode is a Dirichlet type zero volt (i.e. grounded), at the cathode the potential boundary condition is a Neumann-type current flux. The cathode potential boundary condition was calculated to be 1.73 mV/cm at 1C given the geometry modeled and an electronic conductivity of the cathode equal to 0.38 S/cm.

In order to get a general understanding of the considered conservation equations for mass and charge for both solid and electrolyte phase, how the interface between the solid and the electrolyte phase is formulated, which constitutive relations for the transport coefficients are used and how the numerics is designed in OpelLiB please see **[45, 46]**.

Figure 9 shows the simulated discharge curves of the modeled battery cell. At all C-rates, the discharge curves show an early termination, stopping between 35% and 55% of total capacity. This is caused by a lithium concentration build-up at the surface of the rather large cathode particles. The maximum concentration of the material is reached before the ions are able to diffuse through the cathode matrix, as seen in **Figure 10**; this indicates that the battery is solid-phase diffusion limited. When plotted in a similar manner to the lithium concentration distribution, the potential distribution across the particles did not show any gradient.

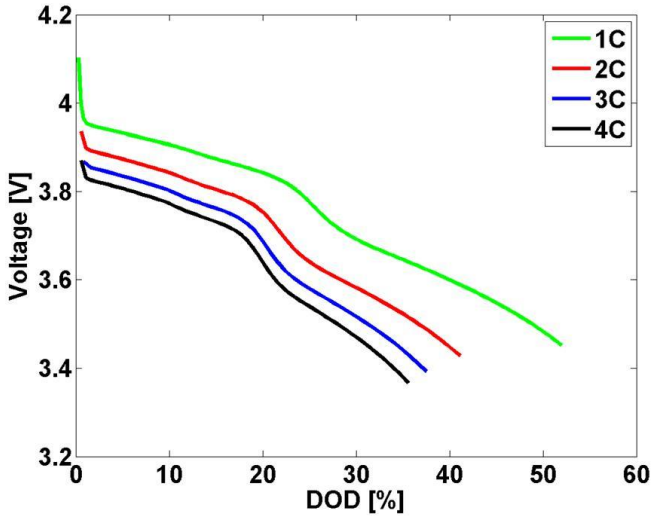

Figure 9: Voltage versus depth of discharge (DOD) results for simulations run at 1C, 2C, 3C and 4C.

The voltage drop at each increasing discharge rate, and the early discharge termination is due to increased ion concentration at the surface of the particle due to diffusion limitations in the solid phase.

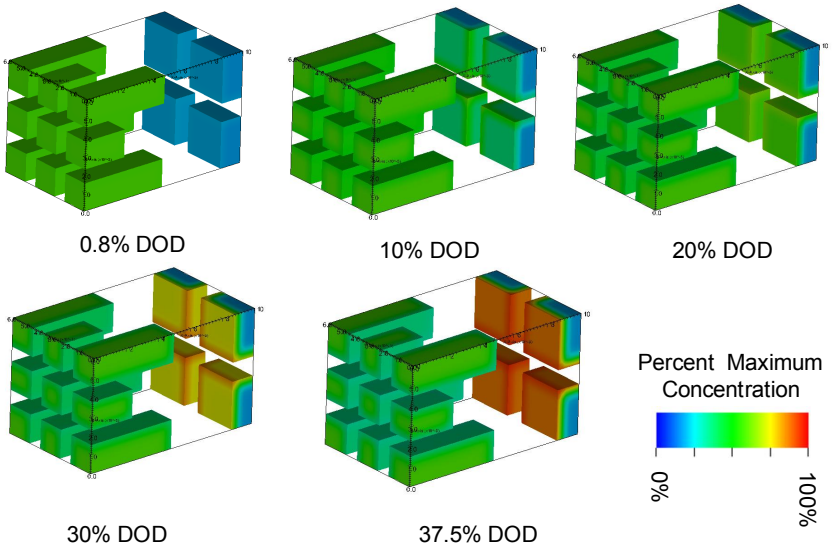

Figure 10: Images of the local distribution of Li concentration in the cell at a 3C discharge rate. At 37.5% depth of discharge (DOD), lithium reaches the end condition of maximum allowable concentration at the surface of the cathode particles.

The voltage plateaus seen in **Figure 9** are typical for low C-rate discharges of lithium manganese oxide spinels. They are observed here at C-rates above 1C because the simulation geometry is closer to that of a single particle directly connected to the current collector than that of a porous composite electrode (i.e. there is no aggregate effect). Real composite electrodes are comprised of aggregated particles exhibiting a percolation network; porous models of composite electrodes which take percolation into account, as well as experimental data, do not show plateaus above 1C. Note that our nominal 1C discharge may in fact be a greater actual discharge rate due to the solid-phase diffusion limit preventing full use of the cathode volume, and thus capacity.

The approach taken here utilizes small, simple and generic electrode structures first and systematically increases structure complexity and domain size later to ensure development of a stable and robust code for industrial code application. Hence, future work aims at utilizing imaging data sets obtained from real electrode samples as shown in **Figure 4**. This is a precondition to walk through the material design cycle as illustrated in **Figure 5**.

The work related to the Li-ion battery electrode simulation as reflected in this chapter has been supported by the Advanced Battery Coalition for Drivetrains (ABCD), a joint effort by General Motors and the University of Michigan **[47]**.

7 Summary and Conclusions

Porous media in electrochemical cells are thin, laterally extended sheets and represent complex assemblies of electrochemically active and non-active composite materials with different pore shapes on different scales of pore size and surface properties. The objective of pore scale modeling is to understand the correlation of pore structure and effective material properties and, eventually, determine and control the macroscopic, effective material properties and cell behavior. For the purpose of improving porous materials of electrochemical cells a general CAE process using virtual materials and physico-chemical transport models has successfully been demonstrated. The process provides fundamental insight into the correlation and interaction between the three-dimensional micro-morphology of the porous material, the physical transport phenomena as well as the electrochemical processes. Teethed with well-designed test methodologies such a CAE methodology provides a strong platform to understand material functionality and degradation mechanisms; a precondition to develop material optimization and/or degradation mitigation strategies. In that regard, such a process envisions a virtual material characterization method where material properties that are difficult to measure in an experiment can be obtained numerically. This also provides predictive capabilities to accelerate and improve the material development.

Major challenges of the described CAE process can be summarized as follows:

- Tomographical imaging techniques for porous materials of electrochemical cells are generally available. The quality of the imaging data sets, though, needs to be improved to enable and/or facilitate the succeeding image processing.
- In composite materials such as the DM (comprised of CFP and MPL) or the positive Li-ion battery electrode (µm-scale active particle and nm-scale binder and conductivity-enhancing additives) imaging cannot provide or resolve all components. This needs to be reflected appropriately by the model.
- The image processing of raw imaging data (in general, the segmentation of gray scale data sets) needs to be further developed to obtain a reliable and distinct identification of solid and void regions.
- Depending on the parameter sensitivity of the model, a comprehensive and accurate parameterization is essential to meet the desired or specified accuracy of the simulation results. This may require improvement of existing or development of new experimental material characterization methods.

- The relationship between material manufacturing parameters and the desired material properties is currently not reflected and will require more future efforts.
- The interaction of adjacent layers with distinct transport properties is not fully understood – the physical processes at the interface need further investigation.
- Due to the small layer thicknesses, the representative elementary volume (REV) may not be met. Detailed studies in that regard are required to transfer accurate effective properties to higher-scale modeling (e.g. cell scale simulation).
- In the fuel cell application, the gas diffusion electrode has not been addressed yet by micro modeling approaches. Specific challenges comprise the existence of both a solid electron and a solid ion conductor, the latter being prone to swelling depending on the interaction with product water. Furthermore, mass transport is occurring in both gas and liquid phase.
- For the Li-ion battery, implementation of the energy equation and consideration of the relevant temperature-dependent mechanisms is missing. Furthermore, gas evolution will generate a two-phase situation that needs to be considered by the model, too.
- Validation of micro scale simulation of the fuel cell CFP has progressed well. However, model validation of the fuel cell MPL and DM assembly as well as the Li-ion battery model is missing.
- The producibility of the virtual material needs to be assured and demonstrated. Therefore, the virtually generated materials need to be realistic from the beginning, and the virtual process may need to model the real manufacturing process.

8 References

[1] R. von Helmolt, U. Eberle: Fuel cell vehicles: Status 2007, Journal of Power Sources 165 (2007) 833–843.

[2] E. Karden, S. Ploumen, B. Fricke, T. Miller, K. Snyder: Energy storage devices for future hybrid electric vehicles, Journal of Power Sources 168 (2007) 2–11.

[3] C. Lim and C.Y. Wang: Effects of hydrophobic polymer content in GDL on power performance of a PEM fuel cell, Electrochemica Acta 49, Issue 24, (2004), p. 4149-4156.

[4] M. Mathias, J. Roth, W. Lehnert, and J. Fleming; Handbook of Fuel Cells - Fundamentals, Technology and Applications, Vol. 3, Chap. 42, Wiley, New York, 2003.

[5] J. T. Gostick, M. W. Fowler, M. A. Ioannidis, M. D. Pritzker, Y. M. Volfkovich and A. Sakars: Capillary pressure and hydrophilic porosity in gas diffusion layers for polymer electrolyte fuel cells, J. Power Sources, 156 (2006) p. 375.

[6] P.R. Shearing, L.E. Howard, P.S. Jørgensen, N.P. Brandon, S.J. Harris, Electrochemistry Communications 12, (2010), 374–377.

[7] R. E. Garcia and Y. M. Chiang, *J. Electrochem. Soc.*, **154**, A856 (2007).

[8] X. C. Zhang, W. Shyy and A. M. Sastry, *J. Electrochem. Soc.*, **154**, A910 (2007).

[9] X. C. Zhang, A. M. Sastry and W. Shyy, *J. Electrochem. Soc.*, **155**, A542 (2008).

[10] C. W. Wang and A. M. Sastry, *J. Electrochem. Soc.*, **154**, A1035 (2007).

[11] P. Arora, R. E. White and M. Doyle, *J. Electrochem. Soc.*, **145**, 3647 (1998).

[12] G. S. Nagarajan, J. W. Van Zee and R. M. Spotnitz, *J. Electrochem. Soc.*, **145**, 771 (1998).

[13] M. Doyle, T. F. Fuller and J. Newman, *J. Electrochem. Soc.*, **140**, 1526 (1993).

[14] L. Berhan and A. M. Sastry, *Physical Review E*, **75** (2007).

[15] L. Berhan and A. M. Sastry, *Physical Review E*, **75** (2007).

[16] Y. H. Chen, S. D. Bakrania, M. S. Wooldridge and A. M. Sastry, *Aerosol Sci. Technol.*, **44**, 83 (2010).

[17] X. Cheng and A. M. Sastry, *Mech. Mater.*, **31**, 765 (1999).

[18] X. Cheng, A. M. Sastry and B. E. Layton, Journal of Engineering Materials and Technology-Transactions of the Asme, **123**, 12 (2001).

[19] A. M. Sastry and C. M. Lastoskie, Philosophical Transactions of the Royal Society of London Series a-Mathematical Physical and Engineering Sciences, **362**, 2851 (2004).

[20] K. A. Striebel, A. Sierra, J. Shim, C. W. Wang and A. M. Sastry, *J. Power Sources*, **134**, 241 (2004).

[21] C. W. Wang, L. Berhan and A. M. Sastry, Journal of Engineering Materials and Technology-Transactions of the Asme, **122**, 450 (2000).

[22] C. W. Wang, K. A. Cook and A. M. Sastry, *J. Electrochem. Soc.*, **150**, A385 (2003).

[23] C. W. Wang and A. M. Sastry, Journal of Engineering Materials and Technology-Transactions of the Asme, **122**, 460 (2000).

[24] C. W. Wang, Y. B. Yi, A. M. Sastry, J. Shim and K. A. Striebel, *J. Electrochem. Soc.*, **151**, A1489 (2004).

[25] Y. B. Yi, L. Berhan and A. M. Sastry, *J. Appl. Phys.*, **96**, 1318 (2004).

[26] Y. B. Yi and A. M. Sastry, *Physical Review E*, **66** (2002).

[27] Y. B. Yi and A. M. Sastry, Proceedings of the Royal Society of London Series a-Mathematical Physical and Engineering Sciences, **460**, 2353 (2004).

[28] Y. B. Yi, C. W. Wang and A. M. Sastry, *J. Electrochem. Soc.*, **151**, A1292 (2004).

[29] Y. B. Yi, C. W. Wang and A. M. Sastry, Journal of Engineering Materials and Technology-Transactions of the Asme, **128**, 73 (2006).

[30] Y. H. Chen, C. W. Wang, X. Zhang and A. M. Sastry, *J. Power Sources*, **195**, 2851 (2010).

[31] W. B. Du, A. Gupta, X. C. Zhang, A. M. Sastry and W. Shyy, *Int. J. Heat Mass Transfer*, **53**, 3552 (2010).

[32] J. H. Seo, J. Park, G. Plett and A. M. Sastry, *Electrochemical and Solid State Letters*, **13**, A135 (2010).

[33] A. Latz, J. Zausch: Thermodynamic consistent transport theory of Li-ion batteries, 195, 2010, http://www.itwm.fraunhofer.de/zentral/download/berichte/bericht_195.pdf

[34] C. Wieser: Nanoporous and Microporous Materials in Fuel Cells, Material Science and Engineering, Congress, Nuremberg, 2008.

[35] C. Wieser, S. Fell, J. Meusinger: Advanced Material Research for Fuel Cells, Edition Ostwald ; Vol. 2, On catalysis, ed. by Wladimir Reschetilowski & Wolfgang Hönle, ISBN 978-3-86135-232-7.

[36] D. Rensink, J. Roth, S. Fell: Liquid Water Transport and Distribution in Fibrous Porous Media and Gas Channels, ASME ICNMM2008-62087, 6th International Conference on Nanochannels, Microchannels and Minichannels, 2008.

[37] T. Berning, C. Wieser, P.-Y. Chuang, T. Trabold: Method for Optimizing Diffusion Media with Spatially Varying Mass Transport Resistance, United States Patent Application Publication, US 2009/0024373 A1.

[38] J. Becker, C. Wieser, D. Fell, K. Steiner: A Multi-Scale Approach to Material Modeling of Fuel Cell Diffusion Media, accepted in Int. J. of Heat and Mass Transfer.

[39] GeoDict, Fraunhofer ITWM 2001-2010, www.geodict.com

[40] J. Becker, V. Schulz, A. Wiegmann: Numerical Determination of Two-Phase Material Parameters of a Gas Diffusion Layer Using Tomography Images, Journal of Fuel Cell Science and Technology, Number 2, Volume 5, pp 21006-21014 (2008).

[41] V.P. Schulz, P.P. Mukherjee, J. Becker, A. Wiegmann und C.Y. Wang: Modeling of Two-phase Behavior in the Gas Diffusion Medium of Polymer Electrolyte Fuel Cells via Full Morphology Approach, Journal of the Electrochemical Society 154, 419-426 (2007).

[42] A. Medalia and F. Heckman: Morphology of Aggregates - II. Size and Shape Factors of Carbon Black Aggregates from Electron Microscopy, Carbon 7 (1969), 567-582.

[43] A. Wiegmann and A. Zemitis, EJ-HEAT: A Fast Explicit Jump harmonic averaging solver for the effective heat conductivity of composite materials, Bericht des Fraunhofer ITWM 94, 2006.

[44] H. Babovsky, On Knudsen Flows within Thin Tubes, J. Stat. Physics 44 (1986), 865-878.

[45] A. Latz, J. Zausch, O. Iliev: Modeling of species and charge transport in Li-ion batteries based on nonequilibrium thermodynamics, 190, 2010, http://www.itwm.fraunhofer.de/zentral/download/berichte/bericht_190.pdf

[46] P. Popov, Y. Vutov, S. Margenov, O. Iliev: Finite volume discretization of equations describing nonlinear diffusion in Li-ion batteries, 191, 2010, http://www.itwm.fraunhofer.de/zentral/download/berichte/bericht_191.pdf

[47] http://abcd.engin.umich.edu/